

Supported Lipid Bilayer Formation from Phospholipid-Fatty Acid Bicellar Mixtures

Tun Naw Sut, Soohyun Park, Bo Kyeong Yoon, Joshua A. Jackman,* and Nam-Joon Cho*

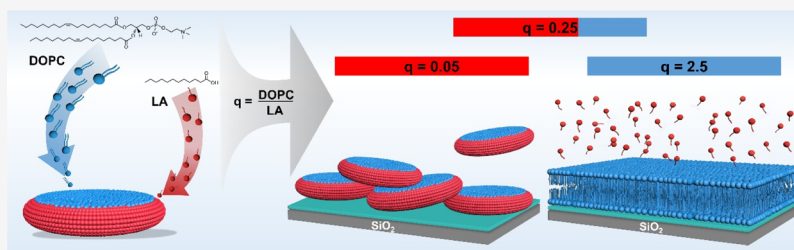
Cite This: *Langmuir* 2020, 36, 5021–5029

Read Online

ACCESS |

Metrics & More

Article Recommendations



ABSTRACT: Supported lipid bilayers (SLBs) are versatile cell membrane-mimicking biointerfaces for various applications such as biosensors and drug delivery systems, and there is broad interest in developing simple, cost-effective methods to achieve SLB fabrication. One promising approach involves the deposition of quasi-two-dimensional bicelle nanostructures that are composed of long-chain phospholipids and either short-chain phospholipids or detergent molecules. While a variety of long-chain phospholipids have been used to prepare bicelles for SLB fabrication applications, only two short-chain phospholipids, 1,2-dihexanoyl-*sn*-glycero-3-phosphocholine and 1,2-diheptanoyl-*sn*-glycero-3-phosphocholine (collectively referred to as DHPC), have been investigated. There remains an outstanding need to identify natural alternatives to DHPC, especially ones that are more affordable, to improve fabrication prospects and application opportunities. Herein, we explored the potential to fabricate SLBs from bicellar mixtures composed of long-chain phospholipids and lauric acid (LA), which is a low-cost, naturally abundant fatty acid that is widely used in soapmaking and various industrial applications. Quartz crystal microbalance-dissipation (QCM-D) experiments were conducted to track bicelle adsorption onto silica surfaces as a function of bicelle composition and lipid concentration, along with time-lapse fluorescence microscopy imaging and fluorescence recovery after photobleaching (FRAP) experiments to further characterize lipid adlayer properties. The results identified optimal conditions where it is possible to efficiently form SLBs from LA-containing bicelles at low lipid concentrations while also unraveling mechanistic insights into the bicelle-mediated SLB formation process and verifying that LA-containing bicelles are biocompatible with human cells for surface coating applications.

INTRODUCTION

Supported lipid bilayers (SLBs) are ultrathin, cell membrane-mimicking interfaces that conformally coat various types of hydrophilic surfaces^{1–3} and are used in a wide range of applications such as biosensors, cell–material interfaces, and drug delivery systems.^{4–9} The bottom-up fabrication of SLBs on a target surface is a classic example of nanoarchitectonics whereby individual phospholipid molecules self-assemble into higher-order, two-dimensional supramolecular structures,^{10–13} which enables the use of highly surface-sensitive measurement techniques for fundamental and applied investigations.^{14–16} To date, the adsorption and spontaneous rupture of lipid vesicles on a solid support—a process termed vesicle fusion—has been the most popular method to fabricate SLBs, although there is ongoing exploration of other SLB fabrication methods.¹⁷

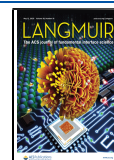
One promising method involves the deposition of bicelles, which are typically viewed as disk-like nanostructured assemblies composed of long-chain and short-chain phospholipid (or detergent) molecules that are concentrated in the

middle bilayer and edge regions, respectively.^{18,19} In actuality, the specific morphology of bicellar mixtures, which are sometimes referred to as bilayered mixed micelles^{20,21} or nanodiscs,²² can encompass disk-like structures as well as other types of nanostructured assemblies, such as worm-like micelles and perforated sheets, depending on factors such as the *q*-ratio (molar ratio of long- to short-chain phospholipids), total lipid concentration, lipid composition, and temperature.^{23–29} While bicelles were originally developed as suitable membrane environments to host transmembrane proteins for structural biology studies,^{20,30–32} they have also proven to be useful tools

Received: March 10, 2020

Revised: April 18, 2020

Published: April 20, 2020



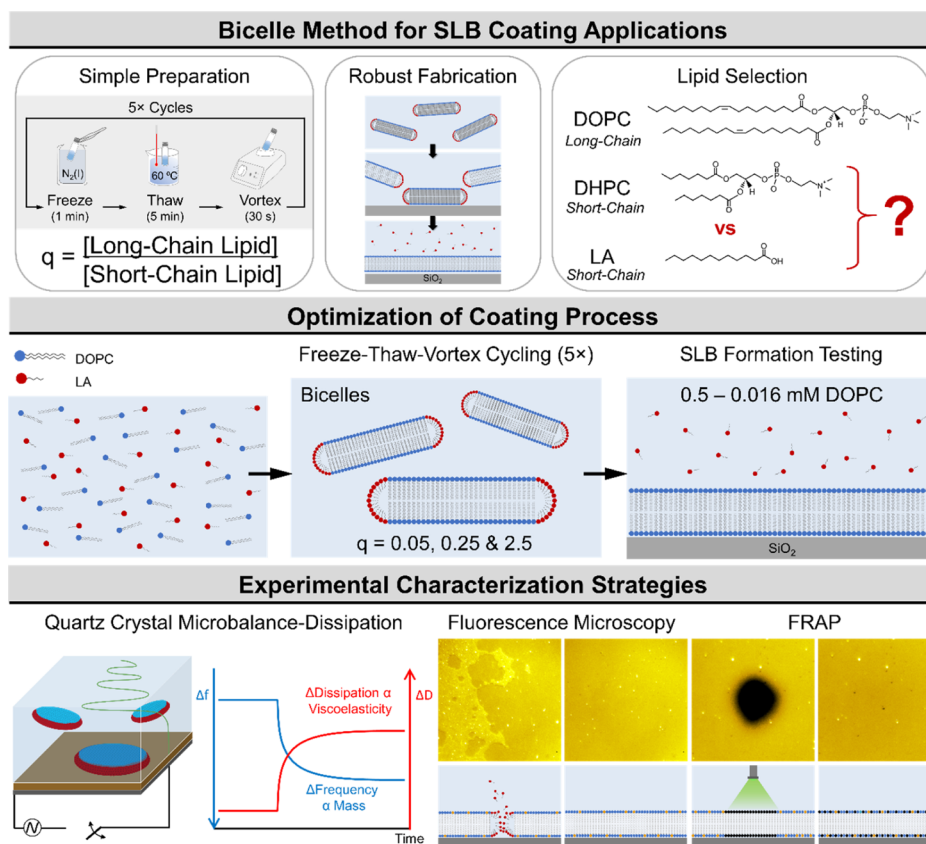


Figure 1. Fabrication strategy: The feasibility of using LA instead of DHPC as the short-chain lipid in bicelles was evaluated for SLB fabrication applications. Bicelle preparation involved hydrating a dry DOPC film in an LA-containing aqueous solution, followed by freeze–thaw–vortex cycling. The SLB formation potential of DOPC/LA bicelles was systematically tested as a function of total lipid concentration and q -ratio. The QCM-D, fluorescence microscopy, and FRAP techniques were employed to characterize bicelle adsorption and resulting SLB formation in applicable cases.

for SLB fabrication, including simplified ones containing zwitterionic phospholipids^{33–36} as well as more complex ones that include various fractions of charged phospholipids^{37,38} or cholesterol,³⁹ and are also useful for micro-patterning applications.⁴⁰ One key advantage of bicelles is that they are easier to prepare than conventionally used vesicles, and the main processing steps involve freeze–thaw–vortex cycling without the need for strict size control.^{17,41} Mechanistically, SLB formation involves bicelle adsorption and fusion on a solid support whereby long-chain phospholipids self-assemble into a conformal SLB while short-chain phospholipids return to the bulk phase.⁴² Depending on the system, it is also possible that bicelles do not adsorb onto a surface or adsorb but remain intact without fusing instead of forming SLBs. Indeed, it has been demonstrated that the effectiveness of bicelle-mediated SLB formation depends on experimental parameters such as total lipid concentration and q -ratio,⁴² along with the substrate type³⁸ and salt concentration.⁴³

To date, a wide range of long-chain phospholipids have been used to make bicelles for successful SLB fabrication, and examples include zwitterionic 1,2-dipalmitoyl-*sn*-glycero-3-phosphocholine (DPPC),³³ 1,2-dimyristoyl-*sn*-glycero-3-phosphocholine (DMPC),³⁴ 1-palmitoyl-2-oleoyl-*sn*-glycero-3-phosphocholine (POPC),³⁵ and 1,2-dioleoyl-*sn*-glycero-3-phosphocholine (DOPC),⁴² positively charged 1,2-dipalmitoyl-*sn*-glycero-3-ethylphosphocholine (DPEPC)³⁷ and 1,2-dioleoyl-*sn*-glycero-3-ethylphosphocholine (DOEPC),³⁸ and negatively

charged 1,2-dipalmitoyl-*sn*-glycero-3-phospho-(1'-*rac*-glycerol) (DPPG)³⁷ and 1,2-dioleoyl-*sn*-glycero-3-phospho-L-serine (DOPS).³⁸ Curiously, however, only two short-chain phospholipids have been used so far, namely 1,2-dihexanoyl-*sn*-glycero-3-phosphocholine (DHPC₆)^{34–37} and 1,2-diheptanoyl-*sn*-glycero-3-phosphocholine (DHPC₇),^{33,35} that are collectively referred to as DHPC herein. The tendency to use DHPC is predicated on its wide usage in solution-phase bicelle studies, in which case the phospholipid structure of DHPC is useful for reconstituting transmembrane properties in a membrane-mimetic environment.⁴⁴ However, other types of detergent-like lipids³¹ and various detergents^{45,46} can also be used to make solution-phase bicelles with desired properties (e.g., enhanced stability^{47,48} and protein activity^{49,50}), and it would be beneficial to explore additional bicelle options for SLB fabrication. Such investigations would expand our mechanistic understanding of the bicelle-mediated SLB formation process beyond DHPC-containing systems alone as well as potentially identify a cheaper alternative to DHPC lipids, which are costly compared to many other lipid-like detergent molecules, for application purposes.⁵¹

Herein, we investigated the potential to fabricate SLBs on silica surfaces by using bicelles composed of DOPC as the long-chain phospholipid and lauric acid (LA) in place of DHPC. LA is a saturated fatty acid with a 12-carbon long hydrocarbon chain and has several advantageous properties, including natural abundance and low cost. Toward this goal, we prepared bicellar mixtures composed of DOPC and LA at

different q -ratios and systematically characterized bicelle adsorption onto silica surfaces, as outlined in Figure 1. We conducted quartz crystal microbalance-dissipation (QCM-D) and time-lapse fluorescence microscopy imaging experiments to track DOPC/LA bicelle adsorption kinetics and to identify conditions where SLB formation occurred. Fluorescence recovery after photobleaching (FRAP) experiments were also performed in order to evaluate lateral lipid diffusion of the lipid adlayers. Taken together, our findings identify suitable conditions where DOPC/LA bicelles can be employed to form high-quality SLBs with suitable mass, viscoelastic, and diffusional properties.

MATERIALS AND METHODS

Reagents. Chloroform solutions of DOPC and 1,2-dioleoyl-*sn*-glycero-3-phosphoethanolamine-*N*-(lissamine rhodamine B sulfonyl) (ammonium salt) (Rh-PE) lipids were purchased from Avanti Polar Lipids (Alabaster, AL, USA). LA was obtained from Sigma-Aldrich (St. Louis, MO). The aqueous solution used in all experiments was 10 mM Tris buffer with 150 mM NaCl (pH 7.5). Buffers and sample solutions were prepared with Milli-Q-treated water (MilliporeSigma, Burlington, MA, USA).

Bicelle Preparation. Bicelles were prepared by lipid hydration, followed by freeze–thaw–vortex cycling, as previously described.⁴² Briefly, DOPC lipids in chloroform were added to a glass vial, and the solvent was evaporated by gentle drying with nitrogen gas and subsequent incubation in a vacuum desiccator overnight. In cases when fluorescence microscopy was used, the DOPC lipids were doped with 0.5 mol % Rh-PE lipids. Next, the dry DOPC film was hydrated to 1 mM in an aqueous solution that contained LA at the following concentrations, 20, 4, and 0.4 mM, in order to make samples with q -ratios of 0.05, 0.25, and 2.5, respectively. The resulting lipid suspensions were then subjected to five freeze–thaw–vortex cycles, which involved the following steps: submersing the sample in liquid nitrogen for 1 min, thawing in a 60 °C water bath for 5 min, and vortexing for 30 s. Immediately before experiment, an aliquot of the stock lipid suspension was diluted in the buffer to the desired final lipid concentration.

Quartz Crystal Microbalance-Dissipation (QCM-D). Bicelle adsorption experiments were conducted using a Q-Sense E4 instrument (Biolin Scientific AB, Stockholm, Sweden). The silica-coated QCM-D sensor chips were repeatedly rinsed with water and ethanol, dried with nitrogen gas, and then treated for 1 min in an oxygen plasma chamber (PDC-002, Harrick Plasma, Ithaca, NY). The temperature of the QCM-D measurement chambers was maintained at 25 °C during experiment. All test solutions were introduced into the measurement chambers under continuous flow conditions by using a peristaltic pump (Reglo Digital MS-4/6, Ismatec, Wertheim, Germany) that was set at a flow rate of 50 μ L/min. Measurement data were collected at multiple odd overtones by the Q-Soft software package (Biolin Scientific AB). The reported data were collected at the fifth overtone and normalized according to the overtone number. Data processing was completed using Q-Tools (Biolin Scientific AB) and OriginPro (OriginLab, Northampton, MA) software programs.

Time-Lapse Fluorescence Microscopy Imaging. Imaging experiments were conducted using a Nikon Eclipse Ti-E inverted microscope with a 60 \times oil-immersion objective (NA 1.49). The excitation source was mercury-fiber illuminator C-HGFIE Intensilight (Nikon, Tokyo, Japan), and the light was passed through a TRITC filter block. An Andor iXon3 897 EMCCD camera was used to record micrograph images at a rate of 1 frame every 3 s. All experiments were conducted within a flow-through microfluidic chamber (sticky-Slide VI 0.4, ibidi GmbH, Martinsried, Germany), and the liquid sample was introduced at a flow rate of 50 μ L/min, as controlled by a peristaltic pump (Reglo Digital MS-4/6). All measurements were conducted at room temperature (\sim 25 °C).

Fluorescence Recovery After Photobleaching (FRAP). Lateral lipid diffusion within adsorbed lipid layers was measured by the FRAP

technique. A single-mode laser with a 532 nm wavelength and 100 mW power intensity (Coherent Inc., Santa Clara, CA) was used to irradiate a 20 μ m diameter region within the adsorbed lipid layer in order to quench the fluorescence signal in this region (“photobleaching”). After laser irradiation was completed, the recovery of fluorescence signal within the bleached region was monitored by recording micrograph images every 2 s for a total of 2 min. Accordingly, the diffusion coefficient of lateral lipid motion was computed using the Hankel transform method.⁵²

Cell Cytotoxicity. The effect of DOPC/LA bicelles (q -ratio of 0.05; 5 mM LA) and free LA (5 mM) on the viability of human immortalized keratinocyte (HaCaT) cells was quantified using a cell-counting kit-8 assay (CCK-8; Dojindo Molecular Technologies, Rockville, MD), according to the manufacturer protocol. In brief, 5000 cells were seeded per well in a 96-well plate (Thermo Fisher Scientific, USA), and the cells were grown overnight in a humidified atmosphere with 5% CO₂ at 37 °C. Then, the cells were treated with DOPC/LA bicelles or free LA and further incubated for 72 h. The negative and positive controls were untreated cells and cells treated with 1% Triton X-100 detergent, respectively. For analysis, the CCK-8 reagent was diluted ten times with culture media and incubated with the cells for 1 h at 37 °C, followed by absorbance measurements at 450 nm wavelength using a plate reader (Infinite 200 PRO microplate reader, Tecan). Prior to the experiment, the cells were maintained in Minimum Essential Medium (MEM; Hyclone) that was supplemented with 10% fetal bovine serum (Hyclone), 100 U mL⁻¹ penicillin (Life Technologies) and 100 mg mL⁻¹ streptomycin (Life Technologies). For the assay, cells were subcultured from the culture flask using a 0.25% Trypsin–EDTA solution (Life Technologies).

RESULTS AND DISCUSSION

Design Strategy. We selected DOPC as the long-chain phospholipid because it can form bicelles,^{53,54} and DOPC/DHPC bicelles have been successfully employed for SLB fabrication.^{38,39,42,43} We selected LA as the short-chain lipid because it is abundant and has an appreciably lower cost than DHPC. For 1 g of material, LA is around 670 times cheaper than DHPC₆ and around 910 times cheaper than DHPC₇. In addition, there have been reports of SLB formation using combinations of DOPC and other detergents such as *n*-dodecyl- β -D-maltoside (DDM).^{55,56} Notably, LA is still around 227 times cheaper than DDM. Thus, LA is a good candidate in terms of natural abundance and cost, and DOPC/LA bicelles were prepared and tested at q -ratios of 0.05, 0.25, and 2.5.

While DOPC/DDM mixtures have been used to form SLBs with time-intensive protocols using a carefully orchestrated series of multiple rinsing steps,^{55,56} we chose to use a more rapid protocol⁴² that has been successfully used with DOPC/DHPC bicelles to form SLBs on silica surfaces under favorable conditions when bicelles adsorb, spontaneously fuse, and DOPC lipids reassemble to form the SLB. In the present study, the DOPC/LA bicelle samples were incubated with the silica surface in order to allow sufficient time for adsorption and any subsequent processes, followed by a single rinsing step with aqueous buffer solution to yield the final lipid adlayer. Below, we describe the experimental results that were obtained when attempting DOPC/LA bicelle-mediated SLB formation on silica surfaces for different total lipid concentrations and q -ratios across three experimental techniques: QCM-D, time-lapse fluorescence microscopy, and FRAP.

Quartz Crystal Microbalance-Dissipation. We performed QCM-D experiments to monitor the real-time adsorption of DOPC/LA bicelles onto silica surfaces, including resulting SLB formation in applicable cases. The QCM-D technique detects the changes in mass and viscoelastic properties of adsorbed lipid films by measuring the shifts in

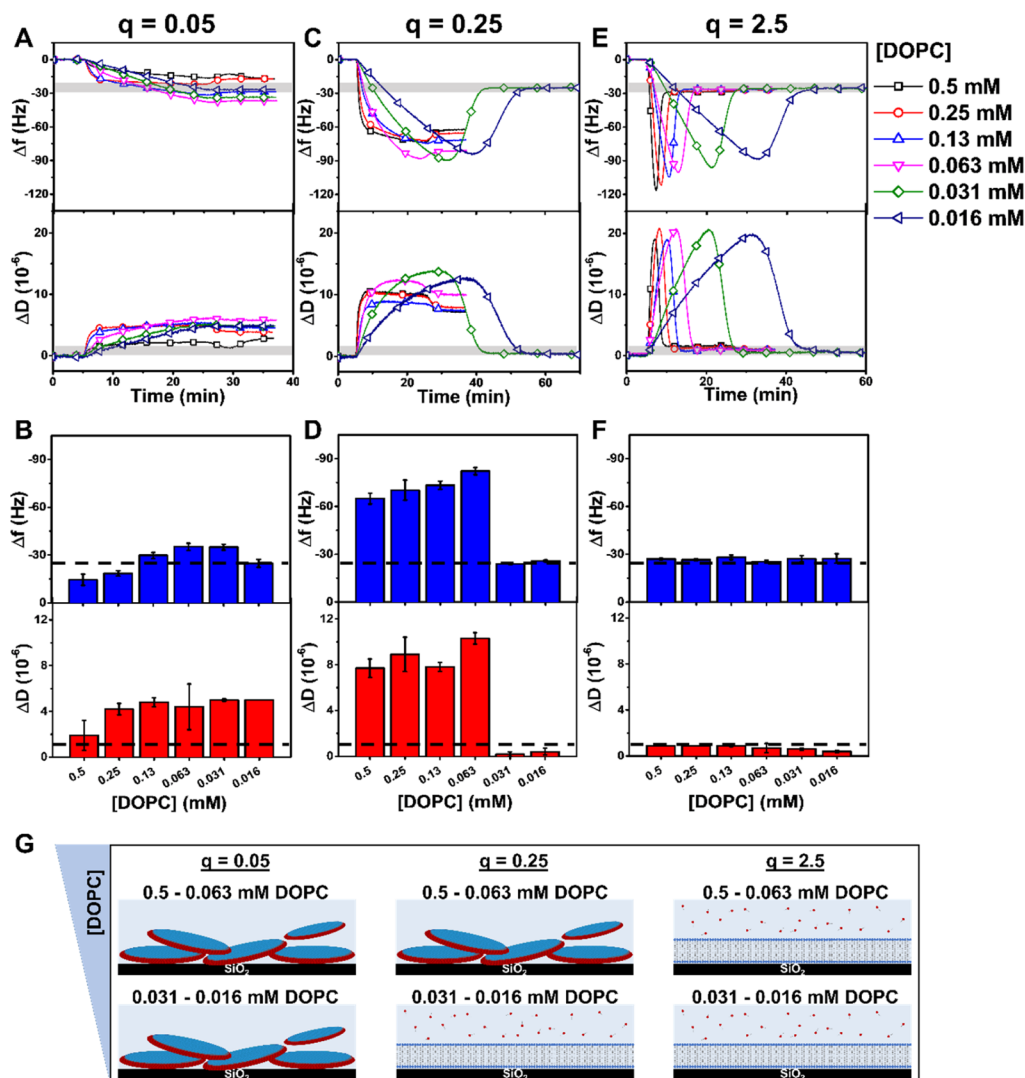


Figure 2. QCM-D characterization of bicelle adsorption onto silica surfaces at different q -ratios. QCM-D Δf and ΔD shifts were recorded as a function of time for bicelle adsorption. (A) Kinetic profiles of Δf (upper panel) and ΔD (lower panel) shifts, and (B) final shifts after buffer wash (upper panel for Δf and lower panel for ΔD) are presented as a function of lipid concentration for bicelles at $q = 0.05$. Corresponding results for bicelle adsorption at (C,D) $q = 0.25$ and (E,F) $q = 2.5$. Highlighted gray regions in the kinetic profiles and the dotted line overlays in the final shift column graphs represent typical measurement values for an SLB. Mean and standard deviations in column graphs are reported from at least three technical replicates. (G) Schematic illustrations of the adsorbed lipid layers at different q -ratios (not drawn to scale).

resonance frequency (Δf) and energy dissipation (ΔD), respectively, of a silica-coated, piezoelectric quartz crystal sensor chip.⁵⁷ The Δf and ΔD shifts were recorded as a function of time, and a baseline signal in aqueous buffer solution was first established within the measurement chamber. Then, the bicelle samples were injected and added under continuous flow until the measurement signals stabilized, followed by a buffer washing step to remove weakly adsorbed lipid molecules. The measurements were stopped after at least 10 min of buffer washing or when the measurement signals reached stable final values. By considering the QCM-D adsorption kinetic profile along with the final Δf and ΔD shifts, it was determined if adsorbing bicelles formed SLBs based on established criteria. Typical values for successful SLB formation corresponded to Δf and ΔD shifts around -26 Hz and less than 1×10^{-6} , respectively.⁵⁷ The QCM-D results are presented as the function of DOPC lipid concentration (with fixed q -ratio) in Figure 2 and discussed below for each q -ratio.

$q = 0.05$. Figure 2A presents the Δf and ΔD shifts for DOPC/LA bicelle adsorption at $q = 0.05$, in which case the LA concentration is 20-fold greater than the DOPC concentration. At 0.5 mM DOPC, there was monotonic adsorption and a washing step led to transient fluctuations until the measurement signal reached final Δf shifts of around -14.5 ± 3.5 Hz and ΔD shift of around $1.9 \pm 1.3 \times 10^{-6}$. Similar results were obtained at 0.25–0.016 mM DOPC with the final Δf shifts ranging around -18 to -35 Hz and the ΔD shifts around 4.2 to 5×10^{-6} . Within the range of 0.5–0.063 mM DOPC, there was a tendency toward greater adsorption uptake at lower lipid concentrations, with maximum uptake observed at 0.063 mM DOPC with final Δf and ΔD corresponding to -35.2 ± 2.2 Hz and $4.4 \pm 2.0 \times 10^{-6}$, respectively (Figure 2B). Altogether, the results demonstrate that DOPC/LA bicelles at $q = 0.05$ adsorb onto silica surfaces but remain intact and do not form SLBs. At this q -ratio, the bicelles in solution are expected to have disk shapes and therefore the adsorbed layers likely consist of discoidal bicelles because bicelles composed of identical or

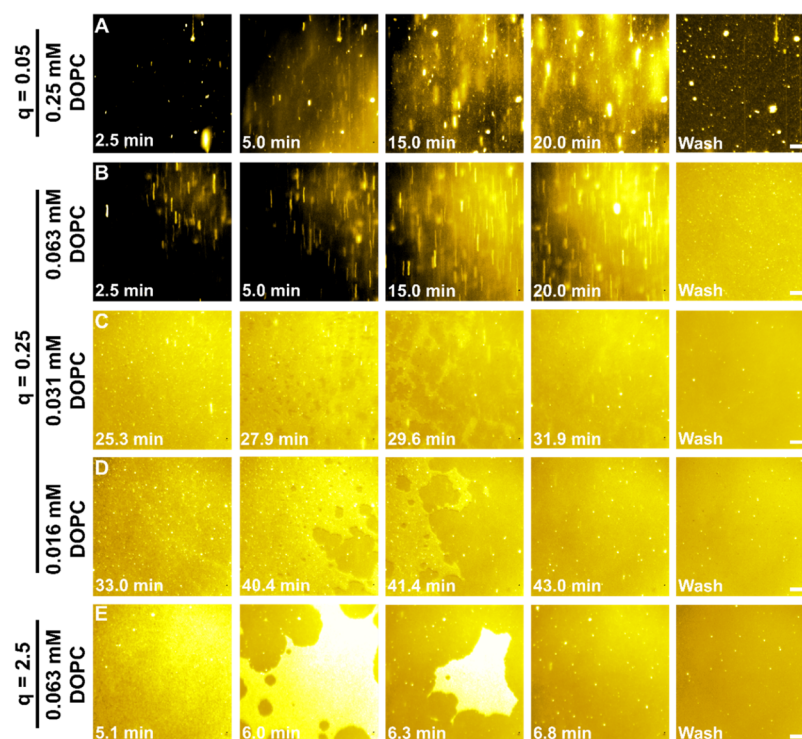


Figure 3. Time-lapse fluorescence microscopy images of bicelle adsorption at different q -ratios. For fluorescence microscopy imaging, bicelles were added onto the glass surface at $t = 0$ min, and the adsorption process was recorded at subsequent time points for the following bicelle cases: $q = 0.05$ at (A) 0.25 mM DOPC; $q = 0.25$ at (B) 0.063 mM DOPC, (C) 0.031 mM DOPC, and (D) 0.016 mM DOPC; and $q = 2.5$ at (E) 0.063 mM DOPC. All scale bars are 20 μm .

similar long-chain lipids with gel-to-fluid phase transition temperatures well below room temperature [e.g., DOPC and DLPC (1,2-dilauroyl-*sn*-glycero-3-phosphocholine)] and short-chain DHPC lipids,⁵³ as well as DMPC/DHPC bicelles⁵⁸ have been reported to exist in disk-like shapes at q -ratios equal to or less than 0.5.

$q = 0.25$. Figure 2C shows the Δf and ΔD shifts for DOPC/LA bicelle adsorption at $q = 0.25$, in which case the LA concentration is fourfold greater than the DOPC concentration. The bicelles adsorbed monotonically at 0.5–0.063 mM DOPC, and the measurement signals stabilized after buffer washing, with Δf and ΔD shifts around -65 to -82 Hz and 7 to 10×10^{-6} , respectively. In contrast, at 0.031 mM DOPC, bicelle adsorption occurred via a two-step mechanism, with final Δf and ΔD values around -25.8 ± 0.6 Hz and $0.4 \pm 0.3 \times 10^{-6}$, respectively. These values are consistent with SLB formation, and the two-step kinetics indicate bicelles adsorb until a critical surface coverage is reached, followed by spontaneous fusion to form an SLB.⁴² At 0.016 mM DOPC, similar results were observed, and the final Δf and ΔD shifts were around -24.0 ± 0.4 Hz and $0.2 \pm 0.2 \times 10^{-6}$, respectively. Figure 2D presents the overall adsorption results at $q = 0.25$. For 0.5–0.063 mM DOPC, the adsorption uptake tended to be slightly greater at lower lipid concentrations. On the other hand, for 0.031 and 0.016 mM DOPC, SLB formation occurred, demonstrating that it is possible to form SLBs from DOPC/LA bicelles under certain conditions. At this q -ratio, the morphology of bicelles in solution is also probably discoidal,^{53,58,59} and hence, the adsorbed layers are presumably composed of bicelle disks while the resulting SLBs are formed through bicelle fusion in which case short-chain LA molecules subsequently return to the bulk solution. SLB

formation at lower total lipid concentrations is consistent with the typical increase in the planar area of bicelle disks as lipid concentrations decrease. Indeed, the aggregation of DMPC/DHPC bicelles at similar q -ratios has been reported at lower lipid concentrations as the short-chain lipid detergent molecules dissociate from bicelles and exist as monomers in the bulk solution.⁵⁸ Accordingly, the larger bicelles formed at lower total lipid concentrations have more contact area with the silica surface and, hence, stronger lipid–substrate interactions, which drives the SLB formation process.³⁸

$q = 2.5$. Figure 2E shows the Δf and ΔD shifts for DOPC/LA bicelle adsorption at $q = 2.5$, in which case the DOPC concentration is 2.5-fold greater than the LA concentration. At all tested concentrations, SLB formation occurred with two-step kinetics indicative of bicelle adsorption and fusion upon reaching a critical surface coverage. As expected, the time span to reach the critical surface coverage was greater at lower lipid concentrations, which is consistent with diffusion-limited adsorption kinetics. The final Δf and ΔD shifts ranged within the SLB values around -25 to -28 Hz and 0.4 to 1×10^{-6} , respectively (Figure 2F). Overall, the results demonstrate that SLB formation is favorable at $q = 2.5$ with all concentrations (0.5 mM DOPC and below). As with DOPC/DHPC bicelles⁵⁴ and DMPC/DHPC bicelles⁶⁰ at similar q -ratios, the DOPC/LA bicelles likely exist in a spherical form at $q = 2.5$, which is conducive to the SLB formation process akin to vesicle fusion involving spherical vesicles while the presence of short-chain lipids has also been noted to induce detergent-mediated membrane softening.⁶¹

In summary, bicelles adsorbed but did not rupture at all tested concentrations at $q = 0.05$ and at 0.5–0.063 mM DOPC at $q = 0.25$, whereas SLB formation resulted with 0.031–0.016

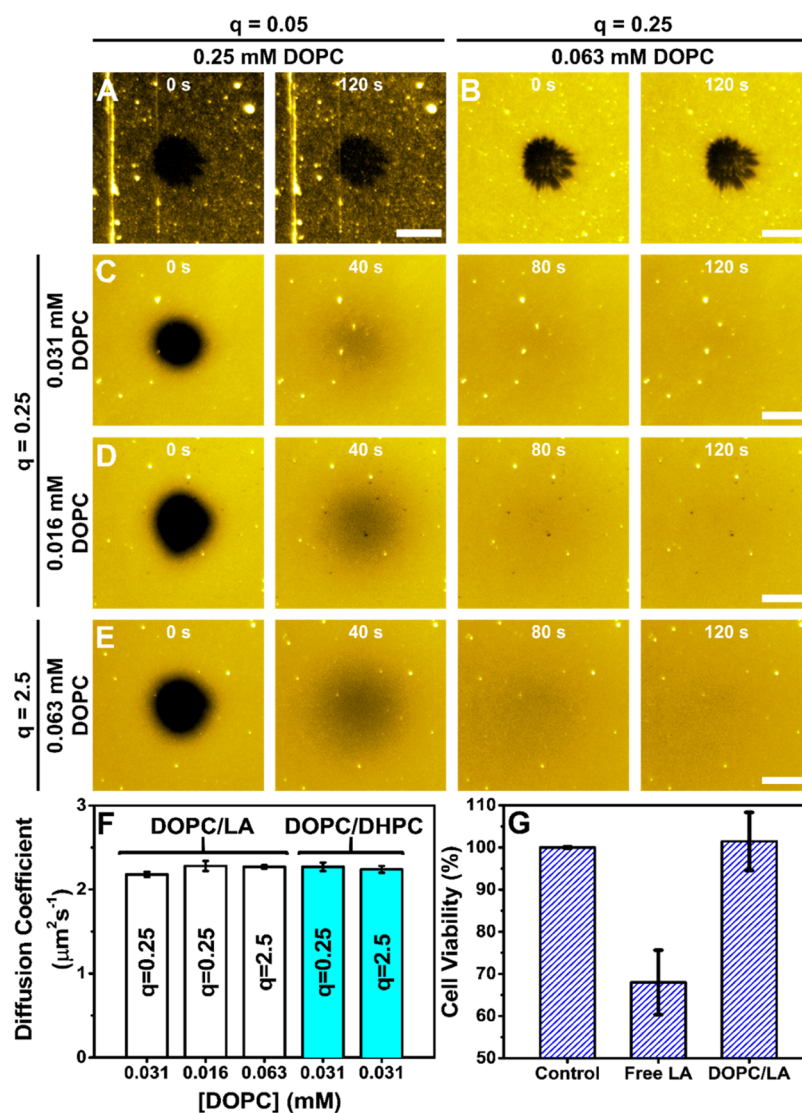


Figure 4. FRAP characterization of adsorbed lipid layers formed from bicelles at different q -ratios. Fluorescence micrographs before and after photobleaching are presented for adsorbed lipid bilayers, which were formed from bicelles with the following conditions: (A) $q = 0.05$ at 0.25 mM DOPC; (B) $q = 0.25$ at 0.063 mM DOPC; (C) $q = 0.25$ at 0.031 mM DOPC; (D) $q = 0.25$ at 0.016 mM DOPC; and (E) $q = 2.5$ at 0.063 mM DOPC. Photobleaching was conducted at $t = 0$ s, and fluorescence recovery within the bleached region was monitored for the next 120 s. All scale bars are 20 μm . (F) Diffusion coefficient values for SLBs formed by DOPC/LA and DOPC/DHPC bicelles with different q -ratios and DOPC lipid concentrations. The DOPC/DHPC data are from ref 42. Mean and standard deviations are reported from six technical replicates. (G) Effect of free LA and DOPC/LA bicelles on cell viability. The LA concentration was fixed at 5 mM, and the bicelle q -ratio was 0.05. Mean and standard deviations are reported from three technical replicates.

mM DOPC at $q = 0.25$ and with all tested concentrations at $q = 2.5$ (Figure 2G).

Time-Lapse Fluorescence Microscopy Imaging. We next performed time-lapse fluorescence microscopy imaging experiments in order to directly observe bicelle adsorption onto silica surfaces. The bicelles were doped with 0.5 mol % of fluorescently labeled Rh-PE lipids (with respect to mol % DOPC), and the DOPC/LA bicelles were added under continuous flow conditions within a microfluidic chamber. The initial injection time was defined as $t = 0$ min, and micrographs at different time points after $t = 0$ min are presented in Figure 3. Based on the QCM-D results, the experimental conditions for fluorescence microscopy experiments were selected to include representative cases at each q -ratio: intact bicelle adsorption at 0.25 mM DOPC for $q = 0.05$; intact bicelle adsorption at 0.063 mM DOPC and SLB

formation at 0.031 and 0.016 mM DOPC for $q = 0.25$; and SLB formation at 0.063 mM DOPC for $q = 2.5$. The corresponding results are discussed below and note that, in cases of SLB formation, the micrographs are presented in a time-lapse sequence whereby the first one corresponds to the onset of SLB formation, that is, at the critical surface coverage.

$q = 0.05$. Despite a relatively high lipid concentration, bicelle adsorption at 0.25 mM DOPC occurred slowly, as evidenced by a gradual change in fluorescence intensity over a 20 min period (Figure 3A). The fluorescence intensity profile of the adsorbed lipid layer exhibited a patchy, nonuniform appearance, with high-intensity lipid aggregates in some regions while there were also significant void regions with negligible adsorption. As such, there was incomplete surface coverage of adsorbed bicelles, which remained intact and did not rupture. Upon a buffer washing step, many of the adsorbed

bicelles were removed from the surface while some remained adsorbed and appeared as bright spots. Together, the data indicate that bicelles adsorbed weakly under this condition, which agrees with the QCM-D data that showed low adsorption uptake.

$q = 0.25$. At 0.063 mM DOPC, bicelles also adsorbed onto the surface and remained intact (Figure 3B). Compared to the bicelle adsorption at $q = 0.05$, a key difference was that most of the adsorbed bicelles remained on the surface after a buffer washing step, as indicated by a nearly uniform fluorescence intensity spanning the surface. In addition, some bright spots indicative of bicellar aggregates were observed. The data further support the QCM-D results that showed greater adsorption uptake but no SLB formation.

In contrast, at 0.031 mM DOPC, bicelle adsorption continued until reaching a critical surface coverage after around 25 min (Figure 3C). At this juncture, adsorbed bicelles fused, and SLB patches began to appear by around 28 min, followed by extensive propagation. SLB formation was completed by around 32 min along with a small number of bright spots likely arising from bicelle aggregates. After a buffer washing step, the SLB remained stably adsorbed on the surface and exhibited a more uniform appearance that is characteristic of high-quality SLBs. At 0.016 mM DOPC, SLB formation occurred in a similar fashion to the 0.031 mM DOPC case, however, it took longer to reach the critical surface coverage (Figure 3D). Thus, DOPC/LA bicelles adsorbed but remained intact at higher lipid concentrations while they adsorbed and fused to form an SLB at lower lipid concentrations.

$q = 2.5$. At 0.063 mM DOPC, bicelle adsorption and resulting SLB formation were noticeably quicker than at the other tested q -ratios despite a relatively low lipid concentration (Figure 3E). A critical surface coverage of adsorbed bicelles was reached at around 5 min. SLB propagation was also rapid, and complete SLB formation was completed within an additional 2 min. Analogous to the SLB cases at $q = 0.25$, a small number of bicelle aggregates appeared in the SLB but were mostly removed after a buffer washing step to yield a high-quality SLB. These findings are also consistent with the QCM-D data, indicating the SLB formation occurs at all tested lipid concentrations for this q -ratio.

Fluorescence Recovery after Photobleaching. The degree of lateral lipid mobility within adsorbed lipid layers was further investigated by FRAP measurements, as presented in Figure 4. Briefly, a small region in the adsorbed lipid layer was photobleached, and fluorescence recovery within the bleached region was measured as neighboring fluorescently labeled lipids diffused into the region. Based on the recovery profile, the diffusion coefficient of lateral lipid mobility within the adsorbed lipid layer was calculated using the Hankel transform method.⁵² Following this approach, it was possible to distinguish adsorbed bicelle layers from SLBs and to determine whether SLBs formed from DOPC/LA bicelles exhibited similar diffusivity profiles to those formed from standard DOPC/DHPC bicelles.

As expected, no fluorescence recovery was observed for adsorbed lipid layers that were prepared using DOPC/LA bicelles with $q = 0.05$ at 0.25 mM DOPC and with $q = 0.25$ at 0.063 mM DOPC (Figure 4A,B). The lack of lateral lipid mobility in these cases is consistent with adsorbed, intact bicelles, and similar results have been previously reported for adsorbed, intact vesicle layers.^{43,62,63}

On the other hand, there were high levels of lateral lipid mobility in all three tested cases corresponding to SLB formation, namely when lipid adlayers were formed from DOPC/LA bicelles with $q = 0.25$ at 0.031 mM DOPC, with $q = 0.25$ at 0.016 mM DOPC, and with $q = 2.5$ at 0.063 mM DOPC (Figure 4C–E). Nearly complete fluorescence recovery occurred within 2 min, and the diffusion coefficients were around $2.2 \mu\text{m}^2/\text{s}$, which indicate the formation of high-quality SLBs (Figure 4F). Notably, the mobility values are also consistent with our past FRAP measurements on SLBs formed from DOPC/DHPC bicelles,⁴² supporting that DOPC/LA bicelles are a useful alternative to form SLBs.

In addition, because free LA is a biologically active molecule with membrane-disruptive properties,⁶⁴ we also evaluated the cell cytotoxicity profiles of 5 mM free LA and 5 mM LA in the form of DOPC/LA bicelles with a q -ratio of 0.05 (Figure 4G). It was observed that DOPC/LA bicelles did not affect viability while treatment with free LA caused $\sim 35\%$ reduction in cell viability. Thus, the DOPC/LA bicelles appear to have suitable properties to serve as a low-cost replacement for DOPC/DHPC bicelles while yielding high-quality SLBs and possessing favorable biocompatibility.

CONCLUSIONS

In this work, we investigated the feasibility of utilizing DOPC/LA bicellar mixtures to fabricate SLBs as an alternative option to conventional DOPC/DHPC bicelles. This direction was motivated by the need to determine if DHPC is the only suitable short-chain lipid for bicelle-mediated SLB formation as well as the practical objective to identify a relatively cheap and natural short-chain lipid or detergent source. Using a combination of surface-sensitive measurement techniques, we identified that DOPC/LA bicelles form SLBs under a range of well-defined conditions. When the LA ratio was very high ($q = 0.05$; 1 DOPC lipid for every 20 LA molecules), SLB formation did not occur. When the LA ratio was moderately high ($q = 0.25$; 1 DOPC lipid for every 4 LA molecules), SLB formation occurred at low total lipid concentrations but not at higher lipid concentrations. In contrast, when the LA ratio was low ($q = 2.5$; 5 DOPC lipids for every 2 LA molecules), SLB formation occurred at all tested concentrations. These findings point to the importance of bicelle nanostructure in influencing the SLB formation process and demonstrate that it is possible to form high-quality SLBs from LA-rich bicellar systems at low total lipid concentrations. Aside from improving our scientific understanding of the bicelle-mediated SLB formation process, such findings open the door to low-cost SLB fabrication with simple preparation methods and widely available lipid components to expand the use of SLB platforms for various applications.

AUTHOR INFORMATION

Corresponding Authors

Joshua A. Jackman – School of Chemical Engineering,
Sungkyunkwan University, Suwon 16419, Republic of Korea;
 orcid.org/0000-0002-1800-8102; Email: jjackman@skku.edu

Nam-Joon Cho – School of Materials Science and Engineering,
Nanyang Technological University, 639798, Singapore;
 orcid.org/0000-0002-8692-8955; Email: njcho@ntu.edu.sg

Authors

Tun Naw Sut – School of Materials Science and Engineering, Nanyang Technological University, 639798, Singapore; School of Chemical Engineering, Sungkyunkwan University, Suwon 16419, Republic of Korea

Soohyun Park – School of Materials Science and Engineering, Nanyang Technological University, 639798, Singapore;

orcid.org/0000-0003-3261-7585

Bo Kyeong Yoon – School of Chemical Engineering, Sungkyunkwan University, Suwon 16419, Republic of Korea

Complete contact information is available at:

<https://pubs.acs.org/10.1021/acs.langmuir.0c00675>

Notes

The authors declare no competing financial interest.

ACKNOWLEDGMENTS

This work was supported by the National Research Foundation of Singapore through a Proof-of-Concept grant (NRF2015NRF-POC0001-19). In addition, this work was supported by the Korea Research Fellowship Program through the National Research Foundation of Korea (NRF) funded by the Ministry of Science and ICT (2019H1D3A1A01070318). The authors thank P. Tanguturi for technical assistance with cell cytotoxicity experiments.

REFERENCES

(1) Hardy, G. J.; Nayak, R.; Zauscher, S. Model Cell Membranes: Techniques to Form Complex Biomimetic Supported Lipid Bilayers via Vesicle Fusion. *Curr. Opin. Colloid Interface Sci.* **2013**, *18*, 448–458.

(2) Jackman, J. A.; Tabaei, S. R.; Zhao, Z.; Yorulmaz, S.; Cho, N.-J. Self-Assembly Formation of Lipid Bilayer Coatings on Bare Aluminum Oxide: Overcoming the Force of Interfacial Water. *ACS Appl. Mater. Interfaces* **2015**, *7*, 959–968.

(3) Su, H.; Liu, H.-Y.; Pappa, A.-M.; Hidalgo, T. C.; Cavassin, P.; Inal, S.; Owens, R. M.; Daniel, S. Facile Generation of Biomimetic-Supported Lipid Bilayers on Conducting Polymer Surfaces for Membrane Biosensing. *ACS Appl. Mater. Interfaces* **2019**, *11*, 43799–43810.

(4) Bally, M.; Bailey, K.; Sugihara, K.; Grieshaber, D.; Vörös, J.; Städler, B. Liposome and Lipid Bilayer Arrays towards Biosensing Applications. *Small* **2010**, *6*, 2481–2497.

(5) Mazur, F.; Bally, M.; Städler, B.; Chandrawati, R. Liposomes and Lipid Bilayers in Biosensors. *Adv. Colloid Interface Sci.* **2017**, *249*, 88–99.

(6) Kuo, C.-J.; Chiang, H.-C.; Tseng, C.-A.; Chang, C.-F.; Ulaganathan, R. K.; Ling, T.-T.; Chang, Y.-J.; Chen, C.-C.; Chen, Y.-R.; Chen, Y.-T. Lipid-Modified Graphene-Transistor Biosensor for Monitoring Amyloid- β Aggregation. *ACS Appl. Mater. Interfaces* **2018**, *10*, 12311–12316.

(7) Lee, I.-C.; Wu, Y.-C. Assembly of Polyelectrolyte Multilayer Films on Supported Lipid Bilayers to Induce Neural Stem/Progenitor Cell Differentiation into Functional Neurons. *ACS Appl. Mater. Interfaces* **2014**, *6*, 14439–14450.

(8) Lee, I.-C.; Liu, Y.-C.; Tsai, H.-A.; Shen, C.-N.; Chang, Y.-C. Promoting the Selection and Maintenance of Fetal Liver Stem/Progenitor Cell Colonies by Layer-by-Layer Polypeptide Tethered Supported Lipid Bilayer. *ACS Appl. Mater. Interfaces* **2014**, *6*, 20654–20663.

(9) Li, X.; Wang, X.; Sha, L.; Wang, D.; Shi, W.; Zhao, Q.; Wang, S. Thermosensitive Lipid Bilayer-Coated Mesoporous Carbon Nanoparticles for Synergistic Thermochemotherapy of Tumor. *ACS Appl. Mater. Interfaces* **2018**, *10*, 19386–19397.

(10) Ariga, K.; Leong, D. T.; Mori, T. Nanoarchitectonics for Hybrid and Related Materials for Bio-Oriented Applications. *Adv. Funct. Mater.* **2018**, *28*, 1702905.

(11) Ariga, K.; Watanabe, S.; Mori, T.; Takeya, J. Soft 2D Nanoarchitectonics. *NPG Asia Mater.* **2018**, *10*, 90–106.

(12) Komiyama, M.; Yoshimoto, K.; Sisido, M.; Ariga, K. Chemistry Can Make Strict and Fuzzy Controls for Bio-Systems: DNA Nanoarchitectonics and Cell-Macromolecular Nanoarchitectonics. *Bull. Chem. Soc. Jpn.* **2017**, *90*, 967–1004.

(13) Ariga, K.; Mori, T.; Li, J. Langmuir Nanoarchitectonics from Basic to Frontier. *Langmuir* **2018**, *35*, 3585–3599.

(14) Jackman, J. A.; Ferhan, A. R.; Cho, N.-J. Surface-Based Nanoplasmonic Sensors for Biointerfacial Science Applications. *Bull. Chem. Soc. Jpn.* **2019**, *92*, 1404–1412.

(15) Jackman, J. A.; Rahim Ferhan, A.; Cho, N.-J. Nanoplasmonic Sensors for Biointerfacial Science. *Chem. Soc. Rev.* **2017**, *46*, 3615–3660.

(16) Mashaghi, A.; Mashaghi, S.; Reviakine, I.; Heeren, R. M. A.; Sandoghdar, V.; Bonn, M. Label-Free Characterization of Biomembranes: From Structure to Dynamics. *Chem. Soc. Rev.* **2014**, *43*, 887–900.

(17) Jackman, J. A.; Cho, N.-J. Supported Lipid Bilayer Formation: Beyond Vesicle Fusion. *Langmuir* **2020**, *36*, 1387–1400.

(18) Ram, P.; Prestegard, J. H. Magnetic Field Induced Ordering of Bile Salt/Phospholipid Micelles: New Media for NMR Structural Investigations. *Biochim. Biophys. Acta, Biomembr.* **1988**, *940*, 289–294.

(19) Marcotte, I.; Auger, M. I. Bicycles as Model Membranes for Solid-and Solution-State NMR Studies of Membrane Peptides and Proteins. *Concepts Magn. Reson., Part A* **2005**, *24*, 17–37.

(20) Dürr, U. H.; Gildenberg, M.; Ramamoorthy, A. The Magic of Bicycles Lights up Membrane Protein Structure. *Chem. Rev.* **2012**, *112*, 6054–6074.

(21) Caldwell, T. A.; Baoukina, S.; Brock, A. T.; Oliver, R. C.; Root, K. T.; Krueger, J. K.; Glover, K. J.; Tieleman, D. P.; Columbus, L. Low-Q Bicycles Are Mixed Micelles. *J. Phys. Chem. Lett.* **2018**, *9*, 4469–4473.

(22) Hu, A.; Fan, T.-H.; Katsaras, J.; Xia, Y.; Li, M.; Nieh, M.-P. Lipid-Based Nanodiscs as Models for Studying Mesoscale Coalescence – A Transport Limited Case. *Soft Matter* **2014**, *10*, 5055–5060.

(23) Nieh, M.-P.; Raghunathan, V. A.; Glinka, C. J.; Harroun, T. A.; Pabst, G.; Katsaras, J. Magnetically Alignable Phase of Phospholipid “Bicelle” Mixtures Is a Chiral Nematic Made up of Wormlike Micelles. *Langmuir* **2004**, *20*, 7893–7897.

(24) Katsaras, J.; Harroun, T. A.; Pencer, J.; Nieh, M.-P. “Bicellar” Lipid Mixtures as Used in Biochemical and Biophysical Studies. *Naturwissenschaften* **2005**, *92*, 355–366.

(25) Harroun, T. A.; Koslowsky, M.; Nieh, M.-P.; de Lannoy, C.-F.; Raghunathan, V. A.; Katsaras, J. Comprehensive Examination of Mesophases Formed by DMPC and DHPC Mixtures. *Langmuir* **2005**, *21*, 5356–5361.

(26) van Dam, L.; Karlsson, G.; Edwards, K. Morphology of Magnetically Aligning DMPC/DHPC Aggregates Perforated Sheets, Not Disks. *Langmuir* **2006**, *22*, 3280–3285.

(27) Pabst, G.; Kučerka, N.; Nieh, M.-P.; Rheinstädter, M. C.; Katsaras, J. Applications of Neutron and X-Ray Scattering to the Study of Biologically Relevant Model Membranes. *Chem. Phys. Lipids* **2010**, *163*, 460–479.

(28) Nieh, M.-P.; Raghunathan, V. A.; Pabst, G.; Harroun, T.; Nagashima, K.; Morales, H.; Katsaras, J.; Macdonald, P. Temperature Driven Annealing of Perforations in Bicellar Model Membranes. *Langmuir* **2011**, *27*, 4838–4847.

(29) Li, M.; Morales, H. H.; Katsaras, J.; Kučerka, N.; Yang, Y.; Macdonald, P. M.; Nieh, M.-P. Morphological Characterization of DMPC/CHAPSO Bicellar Mixtures: A Combined SANS and NMR Study. *Langmuir* **2013**, *29*, 15943–15957.

(30) van Dam, L.; Karlsson, G.; Edwards, K. Direct Observation and Characterization of DMPC/DHPC Aggregates under Conditions Relevant for Biological Solution NMR. *Biochim. Biophys. Acta, Biomembr.* **2004**, *1664*, 241–256.

- (31) Dürr, U. H. N.; Soong, R.; Ramamoorthy, A. When Detergent Meets Bilayer: Birth and Coming of Age of Lipid Bicelles. *Prog. Nucl. Magn. Reson. Spectrosc.* **2013**, *69*, 1.
- (32) De Angelis, A. A.; Opella, S. J. Bicelle Samples for Solid-State NMR of Membrane Proteins. *Nat. Protoc.* **2007**, *2*, 2332.
- (33) Zeineldin, R.; Last, J. A.; Slade, A. L.; Ista, L. K.; Bisong, P.; O'Brien, M. J.; Brueck, S. R. J.; Sasaki, D. Y.; Lopez, G. P. Using Bicellar Mixtures to Form Supported and Suspended Lipid Bilayers on Silicon Chips. *Langmuir* **2006**, *22*, 8163–8168.
- (34) Tabaei, S. R.; Jönsson, P.; Brändén, M.; Höök, F. Self-Assembly Formation of Multiple DNA-Tethered Lipid Bilayers. *J. Struct. Biol.* **2009**, *168*, 200–206.
- (35) Morigaki, K.; Kimura, S.; Okada, K.; Kawasaki, T.; Kawasaki, K. Formation of Substrate-Supported Membranes from Mixtures of Long- and Short-Chain Phospholipids. *Langmuir* **2012**, *28*, 9649–9655.
- (36) Saleem, Q.; Zhang, Z.; Petretic, A.; Gradinaru, C. C.; Macdonald, P. M. Single Lipid Bilayer Deposition on Polymer Surfaces Using Bicelles. *Biomacromolecules* **2015**, *16*, 1032–1039.
- (37) Yamada, N. L.; Sferazza, M.; Fujinami, S. In-Situ Measurement of Phospholipid Nanodisk Adhesion on a Solid Substrate Using Neutron Reflectometry and Atomic Force Microscopy. *Phys. B* **2018**, *551*, 222–226.
- (38) Sut, T. N.; Jackman, J. A.; Cho, N.-J. Understanding How Membrane Surface Charge Influences Lipid Bicelle Adsorption onto Oxide Surfaces. *Langmuir* **2019**, *35*, 8436–8444.
- (39) Sut, T. N.; Park, S.; Choe, Y.; Cho, N.-J. Characterizing the Supported Lipid Membrane Formation from Cholesterol-Rich Bicelles. *Langmuir* **2019**, *35*, 15063–15070.
- (40) Belling, J. N.; Cheung, K. M.; Jackman, J. A.; Sut, T. N.; Allen, M.; Park, J. H.; Jonas, S. J.; Cho, N.-J.; Weiss, P. S. Lipid Bicelle Micropatterning Using Chemical Lift-Off Lithography. *ACS Appl. Mater. Interfaces* **2020**, *12*, 13447.
- (41) Jackman, J. A.; Zhao, Z.; Zhdanov, V. P.; Frank, C. W.; Cho, N.-J. Vesicle Adhesion and Rupture on Silicon Oxide: Influence of Freeze–Thaw Pretreatment. *Langmuir* **2014**, *30*, 2152–2160.
- (42) Kolahdouzan, K.; Jackman, J. A.; Yoon, B. K.; Kim, M. C.; Johal, M. S.; Cho, N.-J. Optimizing the Formation of Supported Lipid Bilayers from Bicellar Mixtures. *Langmuir* **2017**, *33*, 5052–5064.
- (43) Sut, T. N.; Jackman, J. A.; Yoon, B. K.; Park, S.; Kolahdouzan, K.; Ma, G. J.; Zhdanov, V. P.; Cho, N.-J. Influence of NaCl Concentration on Bicelle-Mediated SLB Formation. *Langmuir* **2019**, *35*, 10658–10666.
- (44) Hauser, H. Short-Chain Phospholipids as Detergents. *Biochim. Biophys. Acta, Biomembr.* **2000**, *1508*, 164–181.
- (45) Rieth, M. D.; Glover, K. J. A Novel Lipid-Polymer System with Unique Properties Has Potential in Drug Delivery and Biotechnology Applications. **2018**, bioRxiv:437327.
- (46) Geisler, R.; Pedersen, M. C.; Hannappel, Y.; Schweins, R.; Prévost, S.; Dattani, R.; Arleth, L.; Hellweg, T. Aescin-Induced Conversion of Gel-Phase Lipid Membranes into Bicelle-Like Lipid Nanoparticles. *Langmuir* **2019**, *35*, 16244–16255.
- (47) Cavagnero, S.; Dyson, H. J.; Wright, P. E. Improved Low pH Bicelle System for Orienting Macromolecules over a Wide Temperature Range. *J. Biomol. NMR* **1999**, *13*, 387–391.
- (48) Wang, H.; Eberstadt, M.; Olejniczak, E. T.; Meadows, R. P.; Fesik, S. W. A Liquid Crystalline Medium for Measuring Residual Dipolar Couplings over a Wide Range of Temperatures. *J. Biomol. NMR* **1998**, *12*, 443–446.
- (49) McKibbin, C.; Farmer, N. A.; Jeans, C.; Reeves, P. J.; Khorana, H. G.; Wallace, B. A.; Edwards, P. C.; Villa, C.; Booth, P. J. Opsin Stability and Folding: Modulation by Phospholipid Bicelles. *J. Mol. Biol.* **2007**, *374*, 1319–1332.
- (50) Czerski, L.; Sanders, C. R. Functionality of a Membrane Protein in Bicelles. *Anal. Biochem.* **2000**, *284*, 327–333.
- (51) Kessi, J.; Poiree, J.-C.; Wehrli, E.; Bachofen, R.; Semenza, G.; Hauser, H. Short-Chain Phosphatidylcholines as Superior Detergents in Solubilizing Membrane Proteins and Preserving Biological Activity. *Biochemistry* **1994**, *33*, 10825–10836.
- (52) Jönsson, P.; Jonsson, M. P.; Tegenfeldt, J. O.; Höök, F. A Method Improving the Accuracy of Fluorescence Recovery after Photobleaching Analysis. *Biophys. J.* **2008**, *95*, 5334–5348.
- (53) Morrison, E. A.; Henzler-Wildman, K. A. Reconstitution of Integral Membrane Proteins into Isotropic Bicelles with Improved Sample Stability and Expanded Lipid Composition Profile. *Biochim. Biophys. Acta, Biomembr.* **2012**, *1818*, 814–820.
- (54) Rodríguez, G.; Rubio, L.; Barba, C.; López-Iglesias, C.; de la Maza, A.; López, O.; Cócera, M. Characterization of New DOPC/DHPC Platform for Dermal Applications. *Eur. Biophys. J.* **2013**, *42*, 333–345.
- (55) Grant, L. M.; Tiberg, F. Normal and Lateral Forces between Lipid Covered Solids in Solution: Correlation with Layer Packing and Structure. *Biophys. J.* **2002**, *82*, 1373–1385.
- (56) Vacklin, H. P.; Tiberg, F.; Thomas, R. K. Formation of Supported Phospholipid Bilayers Via Co-Adsorption with β -D-Dodecyl Maltoside. *Biochim. Biophys. Acta, Biomembr.* **2005**, *1668*, 17–24.
- (57) Cho, N.-J.; Frank, C. W.; Kasemo, B.; Höök, F. Quartz Crystal Microbalance with Dissipation Monitoring of Supported Lipid Bilayers on Various Substrates. *Nat. Protoc.* **2010**, *5*, 1096–1106.
- (58) Glover, K. J.; Whiles, J. A.; Wu, G.; Yu, N.-j.; Deems, R.; Struppe, J. O.; Stark, R. E.; Komives, E. A.; Vold, R. R. Structural Evaluation of Phospholipid Bicelles for Solution-State Studies of Membrane-Associated Biomolecules. *Biophys. J.* **2001**, *81*, 2163–2171.
- (59) Luchette, P. A.; Vetman, T. N.; Prosser, R. S.; Hancock, R. E. W.; Nieh, M.-P.; Glinka, C. J.; Krueger, S.; Katsaras, J. Morphology of Fast-Tumbling Bicelles: A Small Angle Neutron Scattering and NMR Study. *Biochim. Biophys. Acta, Biomembr.* **2001**, *1513*, 83–94.
- (60) Shintani, M.; Matubayasi, N. Morphology Study of DMPC/DHPC Mixtures by Solution-State ^1H , ^{31}P NMR, and NOE Measurements. *J. Mol. Liq.* **2016**, *217*, 62–69.
- (61) Otten, D.; Brown, M. F.; Beyer, K. Softening of Membrane Bilayers by Detergents Elucidated by Deuterium NMR Spectroscopy. *J. Phys. Chem. B* **2000**, *104*, 12119–12129.
- (62) Sugihara, K.; Jang, B.; Schneider, M.; Vörös, J.; Zambelli, T. A Universal Method for Planar Lipid Bilayer Formation by Freeze and Thaw. *Soft Matter* **2012**, *8*, 5525–5531.
- (63) Jackman, J. A.; Kim, M. C.; Zhdanov, V. P.; Cho, N.-J. Relationship between Vesicle Size and Steric Hindrance Influences Vesicle Rupture on Solid Supports. *Phys. Chem. Chem. Phys.* **2016**, *18*, 3065–3072.
- (64) Nakatsuji, T.; Kao, M. C.; Fang, J.-Y.; Zouboulis, C. C.; Zhang, L.; Gallo, R. L.; Huang, C.-M. Antimicrobial Property of Lauric Acid against *Propionibacterium Acnes*: Its Therapeutic Potential for Inflammatory Acne Vulgaris. *J. Invest. Dermatol.* **2009**, *129*, 2480–2488.